

Ferromagnetic resonance and the phase diagrams of the two-dimensional easy-plane ferromagnets $(\text{CH}_3\text{NH}_3)_2\text{CuCl}_4$ and K_2CuF_4

S. O. Demokritov, N. M. Kreines, V. I. Kudinov, and S. V. Petrov

Institute of Physical Problems, USSR Academy of Sciences

(Submitted 21 January 1989)

Zh. Eksp. Teor. Fiz. **95**, 2211–2234 (June 1989)

We have measured ferromagnetic resonance (FMR) in the quasi-two-dimensional easy-plane ferromagnets $(\text{CH}_3\text{NH}_3)_2\text{CuCl}_4$ and K_2CuF_4 for the frequency range 100 to 4500 MHz and temperature range 1.2 to 20 K in various directions of the magnetic field, and have determined H - T phase diagrams for both materials when the magnetic field is perpendicular to the easy-magnetization plane. The results we have obtained can be quantitatively explained in terms of the theory of Berezinskii, Kosterlitz and Thouless, which includes contributions of spin waves and vortices to the destruction of magnetic order.

INTRODUCTION

In the ground-breaking papers of Berezinskii¹ and Kosterlitz and Thouless² the existence of an unusual phase transition (the BKT transition) was predicted in two-dimensional degenerate systems (i.e., the XY -model). At the BKT transition point a new qualitative feature appears in these magnetic systems—rigidity of the in-plane spins relative to rotations. At this point the spin correlation radius goes to infinity; however, long-range order cannot arise in an ideal 2D magnet, and the spontaneous moment equals zero down to $T = 0$ K.^{4,5} This unusual transition is related to the existence of a new type of excitation in planar 2D magnets—magnetic vortices.^{4,5} At low temperatures the vortices are bound in pairs with opposite circulations; below a certain temperature T_{BKT} dissociation of a portion of the vortex pairs occurs, and a phase transition takes place in the system.

The BKT theory in its general form applies to any 2D system with a two-component order parameter.^{4–9} The presence of vortex excitations and the appearance of BKT transitions has been experimentally confirmed in various systems: in films of superfluid helium,^{10–14} in superconducting metallic films,^{15–19} and also in computer experiments.^{20–24} In real quasi-two-dimensional magnets there are always interactions between the layers (although sometimes very small ones), and also some uniaxial in-plane anisotropy (which lowers the degeneracy in the plane). Both these interactions strongly suppress the vortex spin excitations; the character of the BKT transition changes near T_{BKT} , and long-range order develops in the system with $\langle \mathbf{M} \rangle \neq 0$ (Refs. 7,9). Therefore, in quasi-two-dimensional magnets the BKT transition in its “pure” form is difficult to observe. Nevertheless, many characteristic indications of the existence of the BKT transition have been observed in magnetic 2D systems as well.^{25–31}

A system of this type whose magnetic properties have been most thoroughly studied is the quasi-two-dimensional easy-plane ferromagnet (FM) K_2CuF_4 . The measurements given in Ref. 25 of the field dependence of the magnetization in a magnetic field parallel to the easy magnetization plane and the temperature dependence of the paramagnetic susceptibility for K_2CuF_4 showed that the experimental data obtained there could be described quite well within the framework of the BKT theory if the temperature T_{BKT} was taken to be 5.5 K, which was somewhat smaller than the

actual transition temperature $T_c = 6.25$ K. In previous papers^{25,27} it was assumed that the phase transition which occurs in K_2CuF_4 is a BKT transition, although the transition is masked by the appearance of spontaneous magnetization because of the weak interlayer interaction. Later neutron-diffraction investigations of K_2CuF_4 (Refs. 26–28) have confirmed this hypothesis.

In experiments based on quasidelectric neutron scattering in K_2CuF_4 (Ref. 26), determination of the temperature dependence of the in-plane spin correlation radius is based on the width of the magnetic diffraction peaks. In the temperature range $T > 6.6$ K this dependence agrees with the BKT theory with $T_{\text{BKT}} = 5.5$ K. For $T \leq 6.6$ K correlations appear not only in the plane but also in the third dimension (i.e., between layers), leading to the appearance of 3D long-range order.

Investigations of the spin dynamics of K_2CuF_4 by inelastic neutron scattering methods²⁸ attest to the presence in this system of the most interesting characteristic of the BKT transition—the sharp reduction of the frequency of small-wave vector spin waves to zero at the phase transition point. The theory of planar 2D ferromagnets predicts⁸ that the effective exchange constant J_{eff} (a measure of the “rigidity” relative to transverse spin fluctuations, which in turn determines the frequency of the spin waves) should decrease slowly as the temperature increases up to T_{BKT} and then fall sharply to zero at $T = T_{\text{BKT}}$. Of course, this does not imply that there is any change in the microscopic exchange constant. Only the effective spin interaction undergoes a discontinuity, i.e., the gradient energy associated with the mutual orientation of spins at large separations.

Behavior characteristic of a vortex transition in a 2D system with a two-component order parameter was first observed experimentally in planar superfluid helium by Bishop and Reppy,¹⁰ who observed a sharp decrease of the superfluid density (which plays the role of “rigidity” in this system) to zero near the superfluid transition temperature.

The phase transition scenarios for two-dimensional XY -magnets postulated in the BKT theory are also well confirmed in another class of materials, the isomorphic compounds with the general formula $\text{BaM}_2(\text{XO}_4)_2$ ($\text{M} = \text{Co}, \text{Ni}; \text{X} = \text{P}, \text{As}$).^{29–31} This class of antiferromagnets possesses strong XY anisotropy, which confines the spins to planes. For this reason, these 2D antiferromagnets are much closer to the 2D XY model described by the BKT theory than the

Heisenberg 2D ferromagnet K_2CuF_4 , in which the easy-plane anisotropy is weak.

In Ref. 32, it was shown theoretically that in a 2D ferromagnet a magnetic field perpendicular to the easy plane does not immediately destroy the BKT transition, in contrast to the case where the external field lies in the plane. The primary characteristic of the BKT phase transition is the appearance of order with respect to the in-plane spin projection S_{\parallel} ; in this geometry the external field induces a normal component of the magnetic moment M_z , and this moment has no obvious singularities in its field dependence at the transition point. As the field increases, the projection of the spin on the S_{\parallel} plane decreases, and the transition temperature decreases with it so that $T_{BKT} \propto S_{\parallel}^2$. Hence, the H - T phase diagram of a 2D ferromagnet in a magnetic field perpendicular to the easy plane exhibits an entire curve of BKT transitions.³² In Refs. 25, 33 the portion of the phase diagram in the immediate vicinity of $T_c = 6.25$ was determined from magnetic measurements for the compound K_2CuF_4 in this geometry; however, the authors did not present a detailed quantitative description of the data.

In this paper we have used the FMR spectra of the 2D ferromagnets K_2CuF_4 and $(CH_3NH_3)_2CuCl_4$, whose magnetic properties are similar, to determine their phase diagrams over the entire region where in-plane magnetic order exists. We have also been successful in arriving at a quantitative description of our experimental results within the framework of the BKT theory by taking into account the contribution to the destruction of magnetic order from spin waves and vortices (see Sec. IV below).

The plan of this article is as follows: in Sec. I we review the magnetic properties of the compounds K_2CuF_4 and $(CH_3NH_3)_2CuCl_4$, and give a description of our experimental setup. In Sec. II we present the results of our investigations of FMR in an external field perpendicular to the easy-magnetization plane, and determine the phase diagrams of both compounds. In Sec. III we present the results of FMR experiments in which the magnetic field is parallel to the easy-magnetization plane. In Sec. IV the phase diagrams for these FM compounds in a magnetic field perpendicular to the easy-magnetization plane are analyzed within the framework of the BKT theory, taking into account the effect of spin waves. In Sec. V the temperature dependence of various magnetic properties which can be extracted from the FMR spectrum (magnetic moment, FMR frequency in zero field, and in-plane anisotropy) is described using considerations of scale invariance in 2D ferromagnets (theory of similarity).

I. MAGNETIC PROPERTIES OF THE QUASI-TWO-DIMENSIONAL FERROMAGNETS K_2CuF_4 AND $(CH_3NH_3)_2CuCl_4$ AND MEASUREMENT METHODS

The divalent copper compounds $(CH_3NH_3)_2CuCl_4$ (here and in what follows we will always refer to this compound as CuCl1) and K_2CuF_4 are good examples of compounds that can be considered 2D ferromagnets with high accuracy.³⁴⁻³⁸ The compound K_2CuF_4 is a typical 2D ferromagnet with anisotropy of the easy-plane type.³⁷ The magnetic structure of CuCl1 is more complicated, and is discussed in detail in Ref. 39. However, the ordering of the spins in each individual layer of CuCl1 can also be studied by treating the compound as an easy-plane 2D ferromagnet. At

room temperature the compound CuCl1 has a face-centered orthorhombic unit cell with parameters $a_0 = 7.38 \text{ \AA}$, $b_0 = 7.28 \text{ \AA}$, and $c_0 = 18.66 \text{ \AA}$.^{40,41} The structure of K_2CuF_4 is also orthorhombic⁴²; however, its unit cell can be treated as approximately tetragonal with $a_0 = b_0 = 4.155 \text{ \AA}$ and $c_0 = 12.74 \text{ \AA}$.^{37,43}

The magnetic properties of CuCl1 and K_2CuF_4 are similar. For both compounds the ferromagnetic exchange interaction J_0 (and the effective exchange interaction field H_E) between magnetic Cu^{+} ions ($S = 1/2$) within the layers is almost Heisenberg in character. The weak anisotropy A ($\approx 1\%$ of the exchange interaction J_0) tends to "stack" the spins in the basal plane; this anisotropy has a corresponding easy-plane anisotropy field H_A . This easy-plane anisotropy makes these compounds behave at low temperatures like two-dimensional XY ferromagnets of the sort investigated by BKT. However, the very weak exchange interaction J'_0 between planes (with effective field H_e) and the rather small anisotropy in the plane a (H_a) change the character of the BKT transition for CuCl1, so that real crystals exhibit ferromagnetic order below the temperature T_c . By using magneto-optic techniques, the authors of Refs. 44, 45 observed domain structures in both CuCl1 and K_2CuF_4 . The values of the g -factor for K_2CuF_4 and CuCl1 determined from EPR experiments in magnetic fields parallel (g_{\parallel}) and perpendicular (g_z) to the layers are slightly different, i.e., $g_{\parallel} \neq g_z$. These magnetic parameters are well known from a multitude of experiments^{25-28,33-57} and are collected in Table I.

It should be noted that the easy-plane anisotropy A is made up of two parts: A_{exc} , caused by the exchange interaction (between different ions), and A_{dip} , caused by the dipole-dipole interaction: $A = A_{exc} + A_{dip}$ (Refs. 37, 50, 54, 57). The contribution of the dipole forces to the easy-plane anisotropy constant can be calculated rather accurately once the unit-cell parameters are known (see, e.g., Refs. 37, 57). The value of the anisotropy caused by the exchange interaction can be roughly estimated from the anisotropy of the g -factor:

$$A_{exc} \approx \left(\frac{g_{\parallel} - g_z}{g_{\parallel}} \right)^2 J_0.$$

The values of the anisotropy field presented in Table I caused by the exchange interaction $H_{A,exc}$ are found from

$$H_{A,exc} = H_A - H_{A,dip}.$$

In the continuum limit the magnetic properties of the compounds under discussion can be described by the Hamiltonian

$$\mathcal{H} = \int \left\{ \frac{1}{2} J b_0^2 \left[\left(\frac{\partial \mathbf{m}}{\partial x} \right)^2 + \left(\frac{\partial \mathbf{m}}{\partial y} \right)^2 \right] + \frac{1}{2} J' c_0^2 \left(\frac{\partial \mathbf{m}}{\partial z} \right)^2 + \frac{1}{2} A m_z^2 - \frac{1}{2} a m_x^2 - \mathbf{h} \mathbf{m} \right\} \frac{d^2 \mathbf{r}}{b_0^2 c_0}, \quad (1)$$

where \mathbf{m} is a unit vector along the direction of the spins $\mathbf{S}(\mathbf{r})$ at the point \mathbf{r} ; $|\mathbf{m}|^2 = 1$, $\mathbf{h} = g\mu_s S \mathbf{H}$; b_0 , c_0 are the lattice parameters. Here and in what follows the macroscopic exchange interaction constant is $J = \frac{1}{2} S^2 J_0 = 0.5 J_0$ (for a square lattice the number of nearest neighbors in the plane is $z = 4$).

In a previous paper, the authors of Ref. 39 studied the field dependence of the FMR frequency in CuCl1 at the low

TABLE I. Fundamental magnetic characteristics of the easy-plane 2D ferromagnets K_2CuF_4 and $(CH_3NH_3)_2CuCl_4$.

	J_0, K ($H_{E, kOe}$)	$H_A = (H_{A, exc}$ $+ H_{A, dip})$ kOe	J'/J H_c, Oe	H_a, Oe	T_c, K	$M_0, gauss$	$g_{ }$	g_z
K_2CuF_4	$\left\{ \begin{array}{l} 11.2^a \\ 11.4^b \\ 11.93^c \\ (\approx 330) \end{array} \right.$	$\left\{ \begin{array}{l} 2.4^d \\ 2.43^e \\ (1.65 + 0.75)^f \end{array} \right.$	$\left\{ \begin{array}{l} 5 \cdot 10^{-1} \\ (126^d) \end{array} \right.$	$\approx 5^d$	6.25^g	$99^{g, e}$	2.284^h	2.088^h
$(CH_3NH_3)_2CuCl_4$	$\left\{ \begin{array}{l} 19.2^a \\ (\approx 550) \end{array} \right.$	$\left\{ \begin{array}{l} 1.45^d \\ 1.47^e \\ (1.0 + 0.45)^f \end{array} \right.$	$\left\{ \begin{array}{l} 8 \cdot 10^{-5} \\ 45^d \\ 35^e \end{array} \right.$	$\left\{ \begin{array}{l} 84^d \\ 86^e \end{array} \right.$	8.9^g	40^g	2.169^h	2.054^h

^a Measurements of the paramagnetic susceptibility for K_2CuF_4 in Ref. 37, for $(CH_3NH_3)_2CuCl_4$ in Refs. 49, 41.

^b Data from neutron diffraction^{46,47} and heat capacity.⁴⁸

^c Data from inelastic neutron scattering in K_2CuF_4 (Ref. 28).

^d FMR in K_2CuF_4 (Refs. 50–52) and $(CH_3NH_3)_2CuCl_4$ (Ref. 54).

^e Results of present work and Ref. 39.

^f Heat capacity data for K_2CuF_4 (Ref. 37) and $(CH_3NH_3)_2CuCl_4$ (Ref. 55), and also susceptibilities (Ref. 38).

^g Calculation from Refs. 37, 57.

^h Paramagnetic resonance in K_2CuF_4 (Refs. 37, 43, 50–52) and $(CH_3NH_3)_2CuCl_4$ (Refs. 54, 56).

temperature $T = 1.2 \text{ K} \ll T_c$, where fluctuation effects can be neglected. Under these conditions the FMR spectrum is determined only by the magnetic structure of the compound under study and the direction of the field. In order to explain the angular dependence of the FMR spectrum, an unusual ferromagnetic structure was proposed for CuCl1 in Ref. 39, in which the difficult-magnetization axes of the magnetic anisotropy in neighboring planes are directed at an angle to one another.

In this article we present results of an experimental investigation of the temperature dependence of the FMR spectrum for various directions of the magnetic field in CuCl1 and K_2CuF_4 . Measurements of the dependence of the FMR frequency on the external field were carried out in the band of frequencies 100 to 4500 MHz and the temperatures 1.2 to 20 K. The basic topic of discussion in this paper is the investigation of fluctuation-induced features in the FMR spectrum. With this in mind, our experiments were carried out at exceptionally low frequencies and in correspondingly weak magnetic fields, because the application of even a relatively small magnetic field strongly suppresses such short-range fluctuations as vortices and spin waves; this in turn causes the features connected with the two-dimensional character of the system to be much less noticeable or even to disappear entirely. The FMR was measured via absorption of high-frequency power by crystals placed either in a stripline or a helix (i.e., without using a resonator). This enabled us to carry out our measurements over a wide frequency interval (100 to 4500 MHz) within a single experiment. The amount of power fed into the crystals came to less than one mW, while the absorption at resonance was at most 10%. At these levels of microwave power we observed no overheating of the samples at resonance for any temperature. The horizontal magnetic field was produced by an electromagnet into whose gap we placed a helium dewar. By rotating the magnet relative to the vertical axis through an arbitrary angle and rocking it by ± 4 degrees relative to the horizontal axis, we were able to apply the field in the required direction with an accuracy of better than 0.5 degrees. The magnetic field was measured with a Hall apparatus. We installed a system for temperature measurement and stabilization which allowed us to establish and maintain the required temperature within th

experimental volume to an accuracy of 0.1 K. The samples were prepared in the form of thin disks with planes perpendicular to the c_0 axis, with the following dimensions: for CuCl1 $\phi 2.1 \times 0.15$ mm, for K_2CuF_4 $\phi 2.25 \times 0.25$ mm, from which the demagnetization coefficients of the samples equalled $N_z = 4\pi \cdot 0.89$, $N_{||} = 4\pi \cdot 5.3 \cdot 10^{-2}$ and $N_x = 4\pi \cdot 0.85$, $N_{||} = 4\pi \cdot 10^{-2}$, respectively.

The width of the FMR line in the field is rather narrow, amounting to several oersteds in K_2CuF_4 and less than 1 Oe for CuCl1 at $T = 1.2$ K. This attests to the good quality of our samples. As the temperature increased the resonance line broadened.

In order to determine the corrections connected with the demagnetization fields, we carried out measurements of the static magnetization of the samples with a vibrating magnetometer at various temperatures and directions of the magnetic field, both in the plane of the samples and perpendicular to the films.

II. FMR IN A MAGNETIC FIELD PERPENDICULAR TO THE EASY PLANE

In normal easy-plane 3D ferromagnets subjected to a magnetic field directed along the difficult-magnetization axis ($\mathbf{H} \parallel \mathbf{z}$) a spin-reorientation phase transition should be observed: in an external field $H_c = H_A$ the magnetic moment is rotated until it is perpendicular to the easy-magnetization plane (along $\mathbf{H} \parallel \mathbf{z}$) and the FMR frequency in this field vanishes. The field dependence of the FMR spectrum in this case is well-described by the following well-known formulae (see, e.g., Ref. 58):

$$\nu(H) = \gamma(H_a' H_A')^{1/2} \left[1 - \left(\frac{H}{H_A'} \right)^2 \right]^{1/2} \text{ for } H \leq H_A', \quad (2a)$$

$$\nu(H) = \gamma[(H - H_A')(H - H_A' + H_a')]^{1/2} \text{ for } H > H_A', \quad (2b)$$

where

$$H_A' = H_A + (N_z - N_y)M_0, \quad H_a' = H_a + (N_x - N_y)M_0 \approx H_a \quad (2c)$$

for

$$N_{||} = N_x = N_y \ll 1.$$

Here γ is the gyromagnetic ratio. Hence, for easy-plane 3D

ferromagnets in a magnetic field perpendicular to the easy plane, when $H > H_c = H_A$ (this region of fields also will be of fundamental interest to us in what follows) the FMR frequency should follow a simple linear relation when we take into account the anisotropy of the g -factor (see Table I) and the fact that $H_c \ll H_A$:

$$\nu(H) \approx \gamma_z (H_{\text{int}} - H_A), \quad (3a)$$

where

$$H_{\text{int}} = H - (N_z - N_{\parallel}) M_z. \quad (3b)$$

Figure 1 shows the FMR spectra as a function of the internal magnetic field H_{int} in CuCl1 and K_2CuF_4 for $\mathbf{H} \parallel \mathbf{z}$. In converting the external magnetic field of the electromagnet into the internal field of the sample according to Eq.

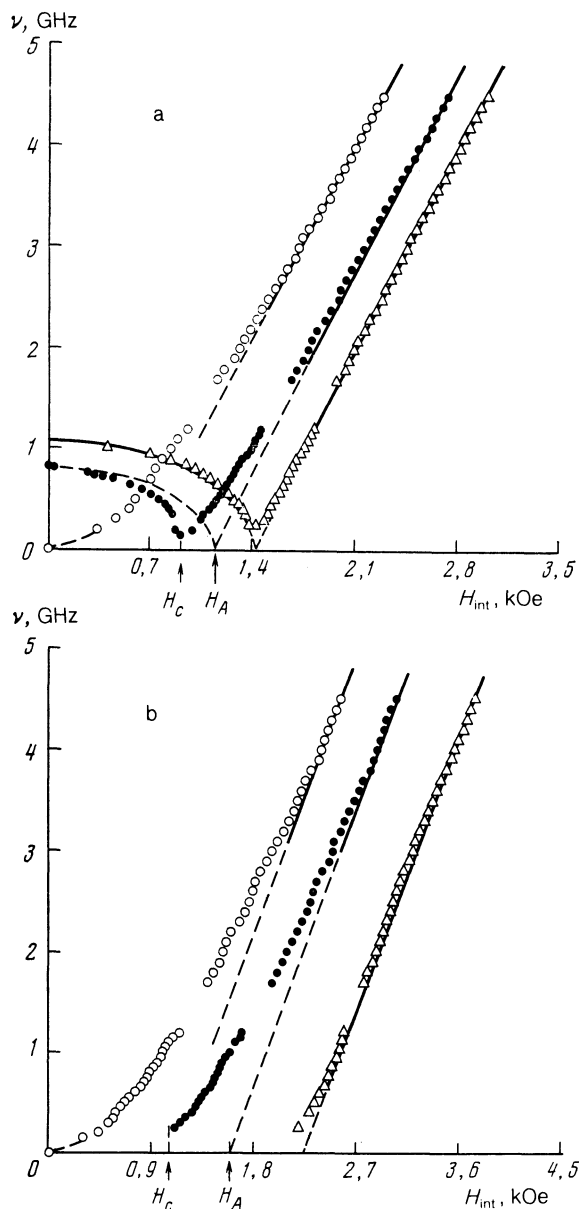


FIG. 1. FMR spectra in a magnetic field perpendicular to the easy axis $\mathbf{H} \parallel \mathbf{z}$ for $(\text{CH}_3\text{NH}_3)_2\text{CuCl}_4$ (a) and K_2CuF_4 (b) at several temperatures: Δ —1.2 K, \bullet —4.2 K, \circ —9 K on (a) and 6.5 K on (b). The curves of $\nu(H)$ were plotted using Eq. (2), with values of $H_A(T)$ chosen for best fit in the region $\nu > 3$ GHz. H_c is the phase transition field while H_A is the easy-plane anisotropy field at $T = 4.2$ K.

(3b), we used values of the demagnetization field which we obtained from a measurement of $M_z(H, T)$ on these same samples. It should be pointed out that based on the magnetic structure of CuCl1 proposed in Ref. 39, the difficult-magnetization axes (and correspondingly the easy-magnetization planes) in neighboring layers should be separated by an angle of $\sim 10^\circ$ from one another. Therefore, if the magnetic field \mathbf{H} is directed parallel to the difficult-magnetization axis for one system of layers, then it will make an angle $\sim 10^\circ$ to the difficult-magnetization axes of the neighboring layers.³⁹ This implies that a FMR measurement will record two resonance peaks. However, in using the $\mathbf{H} \parallel \mathbf{z}$ geometry we are reporting in this paper only resonances associated with those layers for which the external field was directed strictly along the difficult-magnetization axis, which for this case is also taken to define the direction of the z axis.

The orientation of the field of the electromagnet along the direction of the difficult-magnetization axis in the crystals was carried out in two stages at $T = 1.2$ K. Initially, for $H > H_A$ and a fixed frequency of ≈ 3 GHz an external field was applied so that the resonance field was a maximum.³⁹ Then, at lower frequencies down to 100 MHz the field $\mathbf{H} \parallel \mathbf{z}$ was successively oriented more and more precisely so that the FMR frequency was maximally softened in the largest field (which also corresponds to H_A). This procedure allowed us to orient the external field perpendicular to the easy-magnetization plane to an accuracy of better than 0.5° . We note that we did not succeed in reducing the FMR frequency precisely to zero in the critical field $H = H_A$; a gap remained in the resonance spectra corresponding to 100–200 MHz in both the compounds under discussion for $\mathbf{H} \parallel \mathbf{z}$. The value of this gap decreased as the temperature rose. The meaning of this gap is unclear to us.

The FMR spectrum for both materials at the low temperature $T = 1.2$ K is well-described by the usual functions (2), (3) for easy-plane FM (the solid lines in Fig. 1). The different behavior of the resonance spectra of our samples in fields $H \leq H_c$ is connected with the influence of the weak intraplanar anisotropy H_a . Because the compound CuCl1 has the orthorhombic structure with $H_a \neq 0$ (see Table), we observe a gap in the FMR spectrum which at zero field is given by $\nu_0 = \gamma(H_A H_a')^{1/2}$, and which is a minimum at a field $H = H_c$. In the tetragonal compound K_2CuF_4 $H_a \approx 0$ (Ref. 53) and the frequency of uniform oscillations should vanish for $H \leq H_c$. In this region of fields, apparently only those magnetostatic modes with frequencies $\nu \neq 0$ are excited in crystals of K_2CuF_4 ; the frequency of these modes also decreases as the field approaches the phase transition field $H = H_c$. In Fig. 1(b) we show only the FMR spectra of the uniform resonance in K_2CuF_4 .

As the temperature increases the FMR spectrum of both compounds is well-described by the linear dependence (3) with an anisotropy field $H_A(T)$ which depends on temperature in the range of fields $H \gtrsim H_A$ ($T = 0$) (and in the corresponding range of frequencies $\nu \gtrsim 3.5$ GHz). However, in smaller fields (and corresponding frequencies $\nu < 3$ GHz) the function $\nu(H)$ deviates from the linear relation (3) and the FMR frequency reaches a minimum in a field $H = H_c(T)$ smaller than the easy-plane anisotropy field $H_A(T)$ obtained from extrapolation of the high-frequency part of the spectrum according to Eqs. (3).

Thus, in contrast to the usual 3D-ferromagnets, for the

2D ferromagnets under study here the critical field $H_c(T)$ and the anisotropy field $H_A(T)$ differ significantly at finite temperatures.

The temperature dependences $H_A(T)$ and $H_c(T)$, including the contributions from demagnetization, are shown in Fig. 2 for both the compounds under discussion. We suggest that the following picture can describe their behavior in a magnetic field perpendicular to the easy-magnetization plane. Assume that $H_c(T)$ is a curve of phase transitions. Then the value of H_c vanishes at $T = T_c$, and in fields $H \gg H_c(T)$ the order in the plane is destroyed. The order parameter of this transition is the projection of the magnetic moment on the easy-magnetization plane M_{\parallel} : for $H \leq H_c(T)$ we have $M_{\parallel} \neq 0$, while for $H > H_c(T)$ we have $M_{\parallel} = 0$. A second component of the magnetic moment M_z is induced by the external field perpendicular to the plane; in

small fields we should have $M_z = M_0(T)H/H'_A(T)$. At the field $H = H_c(T)$ the spins have a rather large component $S_{\parallel}(\mathbf{r})$ at each point \mathbf{r} ; however, at large spacings these components are disordered and the value of the average projection of the magnetic moment \mathbf{M}_{\parallel} reduces to zero in the critical field. The field dependence $M_z(H)$ has no marked features at the transition point. For $H \gg H_c(T)$ (where $M_{\parallel} = 0$) the spins continue to swing toward the direction of the external field, and the increase in the normal component M_z is practically linear up to a field $H \approx H_A(T)$, at which point it slows sharply. In the range of fields $H > H_A(T)$ the magnetic moment M_z of the sample increases slowly with field, so that it is possible to observe a significant change in the quantity M_z only in the (admittedly wide) interval of fields $H_A \approx 2-3 \text{ kOe} < H < kBT/g\mu BS \approx 100 \text{ kOe}$. The behavior of these two components of the magnetic moment in an external field \mathbf{H} perpendicular to the easy-magnetization plane is illustrated in Fig. 3; in this figure $M_z(H)$ is the component of the magnetization along the field \mathbf{H} measured by us for K_2CuF_4 at $T = 4.2 \text{ K}$, while $M_{\parallel}(H)$ is the hypothetical field dependence of the projection of the magnetization in the plane.

Let us emphasize again that in easy-plane 2D ferromagnets the phase transition field $H_c(T)$ at which $M_{\parallel}(T)$ goes to zero is smaller than the anisotropy field $H_A(T)$, at which the component $M_z(T)$ is close to saturation (Fig. 3). This leads to the circumstance that in 2D-ferromagnets the total value of the magnetic moment is not preserved as it rotates toward the direction of the difficult-magnetization axis with increasing field, i.e., $|\mathbf{M}| \neq \text{const}$. Therefore the phase transition in a magnetic field perpendicular to the easy-magnetization plane takes place not by spin reorientation (which is characteristic of the usual 3D ferromagnets), but rather is an order-disorder transition in the plane.

In contrast to 2D ferromagnets, in 3D ferromagnets the difference between H_c and H_A is small and almost unobservable. It is clear from Fig. 2 that in a 2D ferromagnet the difference between H_c and H_A grows as the temperature increases, and consequently is a fluctuation effect. In addition, we should note that significant departures of the FMR measured spectra of CuCl and K_2CuF_4 from the standard behavior (2), (3) is observed only in the region of relatively small fields $H \lesssim H_A(0)$ (and at the corresponding frequencies $\nu \lesssim 3.5 \text{ GHz}$). The fields required to study FMR at higher frequencies are too large, since a field $H > H_A(0)$ will

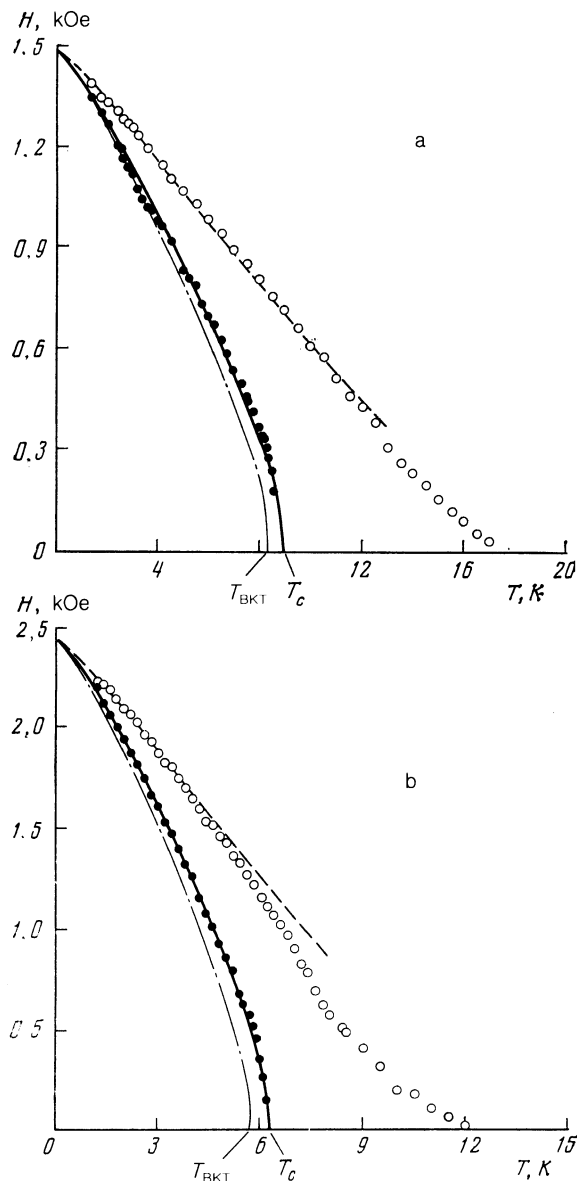


FIG. 2. Temperature dependence of the phase transition field $H_c(T)$ (●) and easy-plane anisotropy field $H_A(T)$ (○) for $(\text{CH}_3\text{NH}_3)_2\text{CuCl}_4$ (a) and K_2CuF_4 (b), obtained from FMR measurements with $\mathbf{H} \parallel \mathbf{z}$: the dashed curves are the theoretical functions $H_A(T)$ [Eq. (13)], the dot-dashed curves are BKT phase transition curves (Eq. 11), and the solid curves are calculated for real phase transitions (see Sec. IV).

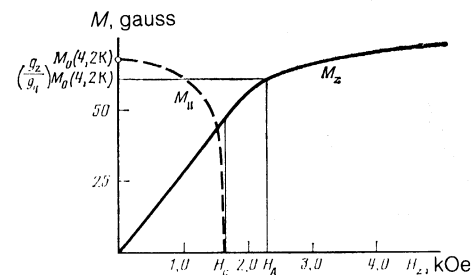


FIG. 3. Field dependence of the two components of the magnetic moment $M_z(T)$ and $M_{\parallel}(T)$ (in the plane) for K_2CuF_4 with $\mathbf{H} \parallel \mathbf{z}$ at $T = 4.2 \text{ K}$. The solid curve is the experimental function $M_z(T)$. The dashed curve is the assumed behavior of the projection of the magnetic moment in the plane; the point $M_0(4.2 \text{ K})$, denoted by ○, is the experimental value of the magnetic moment for $H = 0$ and $T = 4.2 \text{ K}$.

cause the fluctuation features of the two-dimensional behavior to disappear.

The easy-plane anisotropy field $H_A(T)$ (see Fig. 2) has no singularity of any kind at $T = T_c$, so that the curve $H_A(T)$ shown in Fig. 2 does not correspond to any real phase transition in the 2D compounds under study. The effective anisotropy field $H_A(T)$ at which the spins are confined to the plane corresponds to a field in which a reorientation transition should be observable in ordinary 3D ferromagnets. For $T > T_c$ (for which $M_{\parallel} = 0$ for any field in the given geometry) the FMR spectra in 2D ferromagnets preserve their nonlinear form up to those temperatures where H_A becomes insignificant. The anisotropy of the FMR spectra relative to the direction of the magnetic field is preserved up to a temperature of 16 K in CuCl1 and 12 K for K_2CuF_4 , which is significantly higher than the corresponding ferromagnetic transition temperatures $T_c = 8.9$ K and 6.25 K. At these temperatures anisotropy appears in the susceptibility of these compounds^{41,37}; in addition, there is a broad maximum in the temperature dependence of the heat capacity.^{55,37} In neutron experiments on K_2CuF_4 the authors of Refs. 27, 28, 59 observed that short-range spin correlations with a radius on the order of a few lattice spacings are preserved up to 12 K; these authors also observed inelastic neutron scattering by short-wavelength spin waves for $T > T_c$. The existence of a wide temperature range (9–16 K for CuCl1 and 6.3–12 K for K_2CuF_4) in which short-range order exists is undoubtedly a consequence of magnetic 2D interactions in these materials. In 2D magnets the transition to an ordered state often occurs at a temperature significantly smaller than J_0 (19.2 K for CuCl1 and 12 K for K_2CuF_4), whereas the short-range order begins to appear at $T \approx J_0$. This explains the preservation of anisotropy of the magnetic properties in 2D ferromagnets at temperatures which significantly exceed the phase transition temperature T_c .

The temperature dependence of the easy-plane anisotropy field $H_A(T)$ has also been determined previously from the FMR spectrum for CuCl1 (Ref. 54) and for K_2CuF_4 (Refs. 50, 52). However these experiments were carried out in a range of frequencies above 9 GHz, requiring magnetic fields $H \gg H_A$. In our low-frequency experiments we used weaker fields $H \lesssim H_A$; therefore we cannot make any detailed quantitative comparisons, even with respect to overall qualitative agreement, between our results and these earlier investigations involving high-field FMR. Nevertheless it is noteworthy that when extrapolated to $T = 0$ K both the functions H_A and H_c (Fig. 2) reduce to one and the same value $H_A(0) = H_c(0)$, which equals 1480 ± 20 Oe for CuCl1 and 2430 ± 30 Oe for K_2CuF_4 , and the values are close to the data obtained in Refs. 50, 52, 54.

In Ref. 25 (see also Ref. 33) that part of the phase diagram near $T_c = 6.25$ K was determined for K_2CuF_4 from measurements of the temperature dependences of the normal component of the magnetization $M_z(T)$ in a constant field applied along the difficult axis z . The authors of Ref. 25 (see Fig. 4) observed a temperature $T_c(H)$ beyond the phase transition point at which the derivative $(\partial M_z / \partial T)_H$ has a maximum value (the dashed line on Fig. 4). This point on the H - T diagram corresponds to the maximum in the longitudinal susceptibility $\chi_z = (\partial M_z / \partial H_z)_T$ as the magnetic field varies. For comparison, we also show results obtained from our FMR measurements (the solid curve in Fig.

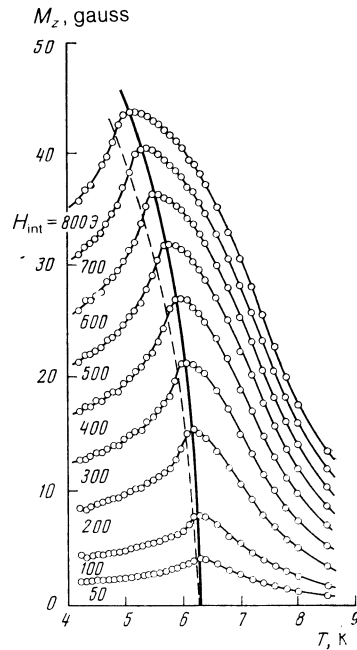


FIG. 4. Temperature dependence of the magnetization component $M_z(T)$ for a constant internal field $H_{int} \parallel z$ for K_2CuF_4 (Fig. 6 from Ref. 25). The dashed curve passes through the maximum values of $(\partial M_z / \partial T)_H$ and corresponds, according to Ref. 25, to a curve of phase transitions $H_c(T)$. The solid curve corresponds to values of the critical field $H_c(T)$ obtained from FMR experiments in this paper.

4). It is clear that with regard to qualitative agreement there are certain quantitative discrepancies: the value of the critical temperature $T_c(H)$ found in our experiments is somewhat larger and corresponds in Fig. 4 to the maximum in the quantity $M_z(T)$ itself rather than its derivative. We do not have an unequivocal explanation of this lack of agreement; nevertheless, we must mention the following facts. As pointed out above, the order parameter for this transition is the projection of the magnetic moment M_{\parallel} in the plane. Consequently, according to the theory of phase transitions⁵ (and in particular, the BKT theory^{4,32}), at the phase transition point the susceptibility $\chi_{\parallel} = (\partial M_{\parallel} / \partial h)$ diverges relative to an infinitesimal field h parallel to the plane. The authors of Refs. 25, 33 measured only the normal component of the magnetic moment M_z , which does not characterize the phase transition in the present case. Therefore the determination of the phase transition temperature in a magnetic field parallel to the difficult-magnetization axis z is indirect with respect to $M_z(T, H)$ and should involve some indeterminacy. Unfortunately, we know of no detailed theoretical investigation of the behavior of the induced field of the magnetic moment component M_z at the phase transition point in a planar 2D ferromagnet.

The theoretical description of the phase diagrams (Fig. 2) will be presented in Sec. IV.

III. FMR SPECTRUM IN A MAGNETIC FIELD PARALLEL TO THE PLANES

(a) $(CH_3NH_3)_2CuCl_4$

In the compound CuCl1 there is a preferred direction of the magnetic moment along an easy-magnetization axis a_0 in every one of the easy-magnetization planes, due to the presence of a weak intralayer anisotropy $H_a = 84$ Oe (see Table

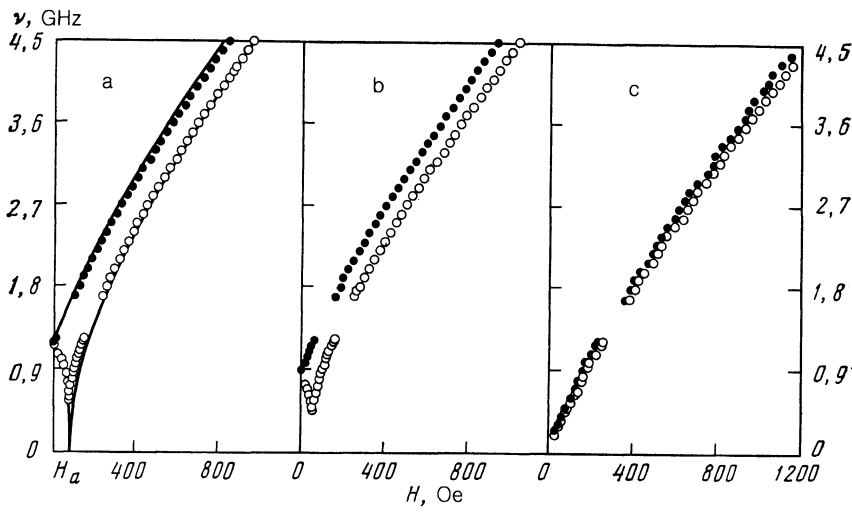


FIG. 5. FMR spectra for $(\text{CH}_3\text{NH}_3)_2\text{CuCl}_4$ at temperatures $T = 1.2$ K (a), 4.2 K (b), and 10 K (c) for two directions of magnetic field \mathbf{H} in the easy magnetization plane ($\mathbf{a}_0, \mathbf{b}_0$): \bullet — $\mathbf{H} \parallel \mathbf{a}_0$, where \mathbf{a}_0 is the easy-magnetization axis; \circ — $\mathbf{H} \parallel \mathbf{b}_0$. The solid curves were obtained using Eq. (4), where H_a is the intraplanar anisotropy field.

1). If the magnetic field is directed along the easy-magnetization plane perpendicular to the axis \mathbf{a}_0 ($\mathbf{H} \parallel \mathbf{b}_0$), a reorientation transition is observed in CuCl1: as the magnetic field increases the magnetic moment \mathbf{M} turns from the axis \mathbf{a}_0 to the axis \mathbf{b}_0 and in fields $H \gg H_0$ it lies strictly along the field \mathbf{H} . In this case the FMR frequency should reduce to zero at the field $H = H_a$. The FMR spectrum of an easy-magnetization FM in the form of a thin disk ($N_x = N_y \gg 1$) for the two directions of the external field in the plane looks as follows^{58,59}: for $\mathbf{H} \parallel \mathbf{a}_0$

$$\nu(H) = \gamma_{\parallel} \left(H_a \frac{g_z}{g_{\parallel}} H_A' \right)^{1/2} \left[1 - \left(\frac{H}{H_a} \right)^2 \right]^{1/2}, \quad H \leq H_a, \quad (4a)$$

$$\nu(H) = \gamma_{\parallel} \left[(H - H_a) \left(H + \frac{g_z}{g_{\parallel}} H_A' - H_a \right) \right]^{1/2}, \quad H > H_a,$$

and for $\mathbf{H} \parallel \mathbf{b}_0$

$$\nu(H) = \gamma_{\parallel} \left[(H + H_a) \left(H + \frac{g_z}{g_{\parallel}} H_A' \right) \right]^{1/2}, \quad (4b)$$

where H_A' was determined earlier from Eq. 2(c).

The measured FMR spectra in CuCl1 for two directions of the in-plane magnetic field $\mathbf{H} \parallel \mathbf{a}_0$ and $\mathbf{H} \parallel \mathbf{b}_0$ are presented in Fig. 5 for several temperatures. At $T = 1.2$ K the solid curves calculated using Eqs. (4) give a good description of the measured resonance spectrum. In the case of $\mathbf{H} \parallel \mathbf{b}_0$ we actually observed a reorientation spin transition at the field $H = H_a$, at which the maximum frequency softens. By using this feature of the field dependence of the FMR spectrum for $\mathbf{H} \parallel \mathbf{b}_0$ we can determine the temperature dependence of the easy-axis anisotropy $H_a(T)$ in the plane. In Fig. 6 we present the results of these measurements of $H_a(T)$. On this same figure we also show the results of the temperature dependence of the FMR frequency ν_0 measured at $H = 0$ in CuCl1. In our samples the demagnetization coefficients along the plane are small, i.e., $N_x = N_y \ll 1$; therefore we can neglect the contribution of the demagnetizing field [see 2(c)]. We note that for $H = H_a$ the resonance frequency does not reduce strictly to zero in this geometry (see Sec. II), i.e., $\mathbf{H} \parallel \mathbf{b}_0$. The remaining gap is estimated to be ≈ 500 MHz at $T = 1.2$ K; as the temperature increases it decreases.

At a temperature $T = T_c$ the anisotropy field H_a in the plane reduces to zero. However, the dependence of the FMR

frequency on the direction of the field in the plane is preserved within a certain region above T_c (see Fig. 5) roughly up to a temperature of 11 K. In this temperature region the anisotropy of the susceptibility within the easy plane is also preserved.⁴¹ On the other hand, the nonlinear character of the dependence of the resonance frequency on magnetic field is preserved up to a temperature of 16 K. This also confirms the presence of an easy-plane anisotropy $H_A \neq 0$ in this temperature region [see (4)], in full agreement with the results of Sec. II.

(b) K_2CuF_4

In the tetragonal crystal K_2CuF_4 (whose magnetic layers form a square lattice) there is no uniaxial (quadratic in \mathbf{M}) in-plane anisotropy. With respect to the angular dependence of the FMR we observed only a weak biquadratic (biaxial) in-plane anisotropy in K_2CuF_4 equal to ≈ 5 Oe at $T = 1.3$ K (Ref. 53). For the case of $H_a = 0$ the resonance frequency does not depend on the direction of the magnetic field in the plane, and Eq. (4) reduces to

$$\nu(H) = \gamma_{\parallel} \left[H \left(H + \frac{g_z}{g_{\parallel}} H_A' \right) \right]^{1/2}. \quad (5a)$$

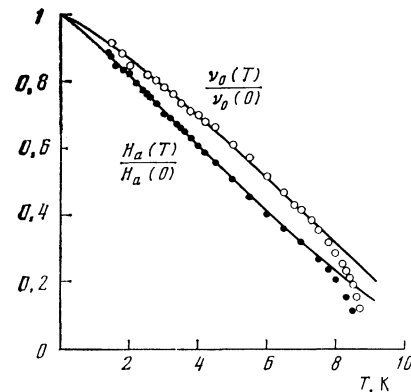


FIG. 6. Temperature dependence of the intraplanar anisotropy field $H_a(T)$ (\bullet) and FMR frequency at $H = 0$ $\nu_0(T)$ (\circ) for $(\text{CH}_3\text{NH}_3)_2\text{CuCl}_4$ in arbitrary units. The solid curves are the result of a calculation using Eqs. (24) and (22) with $H_a(0) = 86$ Oe and $\nu_0(0) = 1240$ MHz.

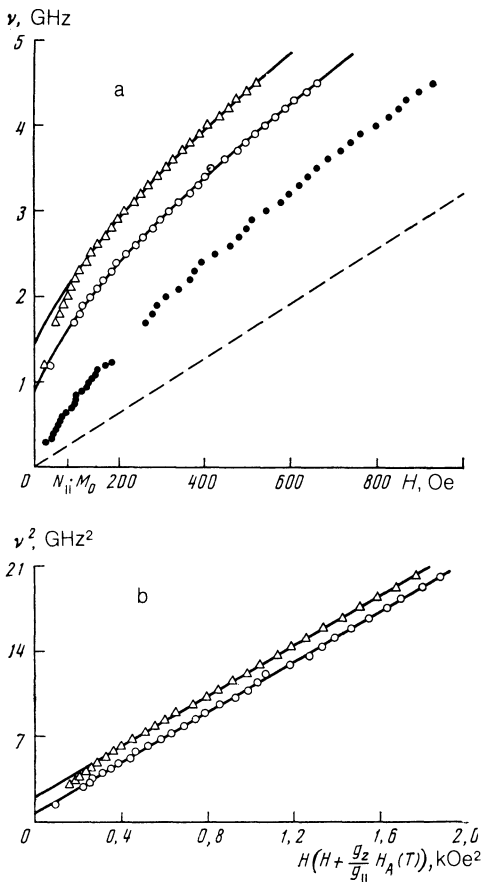


FIG. 7. (a) FMR spectra for K_2CuF_4 for $H \parallel z$ (i.e., in the plane) for several temperatures: Δ —1.2 K, \circ —4.2 K, \bullet —7 K. The dashed curves are paramagnetic resonance curves for $T > 12$ K. The solid curves were obtained from Eq. (5b). (b) FMR spectra for K_2CuF_4 with $H \parallel z$ at 1.2 K (Δ) and 4.2 K (\circ). The straight line is from Eq. (5b).

The measured FMR spectra in K_2CuF_4 in a magnetic field parallel to the plane are shown in Fig. 7(a) for several temperatures. Our experiments showed that to the limits of our accuracy the position of the resonance line does not change as the external field rotates in the easy-magnetization plane, i.e., there is no preferred direction in the plane. However, we did not arrive at a satisfactory description of the measured FMR spectra $\nu(H)$ using the simple function (5a): there is a significant disagreement in the field region $H > 500$ Oe. The experimental data can be brought into good agreement with theory if we admit the possibility of a gap ν_0 being present in the FMR spectrum. The curves in Fig. 7(a), which portray the field dependences of the resonance frequency for this geometry, were calculated using the expression

$$\nu(H) = \left[\nu_0^2 + \gamma_{\parallel}^2 H \left(H + \frac{g_z}{g_{\parallel}} H_A' \right) \right]^{1/2}. \quad (5b)$$

The only quantity which we chose on the basis of a best fit between (5b) and the experimental data was ν_0 ; the quantity H_A in this case was taken from the experiments with $H \parallel z$ (Fig. 2(b)). Using this procedure, we found that the gap in the FMR spectrum came to $\nu_0 = 1370$ MHz at 1.2 K and 830 MHz at 4.2 K.

In Fig. 7(b) we present the experimental data for $\nu(H)$ in terms of the coordinates ν^2 and $H(H + g_z H_A' / g_{\parallel})$. In

these coordinates the resonance spectra [see (5b)] for various temperatures are parallel lines, which intersect on the ordinate axis at a value of the squared FMR frequency ν_0^2 at $H = 0$. We associate the small deviations from the experimental points on Fig. 7 in the region of fields $H \lesssim 90$ Oe with the appearance of a domain structure in the K_2CuF_4 sample. Possible reasons for the observed gap in the FMR spectrum of K_2CuF_4 might be either the magnetoelastic interaction,⁶⁰ or the hyperfine interaction between electrons and the nuclear spins of the Cu^{2+} ions.⁶¹

For $T > T_c$ a nonlinear dependence of the FMR frequency on external field (which indicates that $H_A \neq 0$) is observed at a temperature of ≈ 12 K. In the temperature region $T > 12$ K the resonance spectrum deviates from the paramagnetic law, which also agrees with the results of Ref. 11.

There is still one other interesting feature of FMR in the compound K_2CuF_4 for the geometry in which the external constant field H is directed along planes parallel to the microwave field h , i.e., $H \parallel h \perp z$. As we have already noted, for fields $H < N_{\parallel} M_0(T)$ the sample is found in a multidomain state. When it passes into the single-domain state at $H = N_{\parallel} M_0(T)$ the microwave properties of the crystal, e.g., its longitudinal susceptibility, change sharply. For the case of a microwave signal transmitted along a strip line (in which a crystal of K_2CuF_4 is placed) this results in a feature which appears in the detected microwave power either as a resonance or as a step [Fig. 8(a)]. This feature is most clearly seen in the frequency region 200–600 MHz, where its position with respect to field (corresponding to $H = N_{\parallel} M_0(T)$) is practically independent of frequency. Hence, the presence of this feature in the absorption spectrum for the geometry $H \parallel h$ allowed us to determine the temperature dependence of the field $H = N_{\parallel} M_0(T)$ at which the sample passes into the one-domain state. Once we know the demagnetization coefficient N_{\parallel} of the sample, we can directly find the tempera-

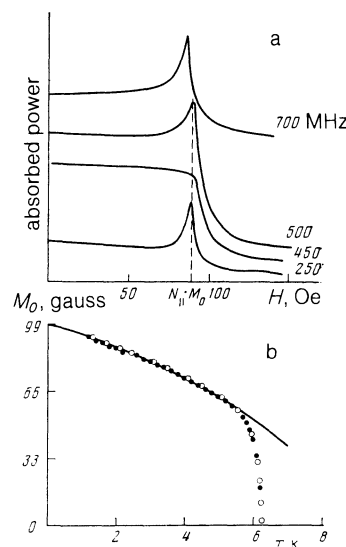


FIG. 8. (a) Microwave absorption curve of K_2CuF_4 in the $H \parallel z$ and $H \parallel h$ geometries, where h is the microwave field at $T = 1.2$ K. $N_{\parallel} M_0$ is the transition field in the single-domain state in the sample. (b) Temperature dependence of the spontaneous magnetic moment $M_0(T)$ for K_2CuF_4 . \bullet —result of measurements of the field $N_{\parallel} M_0(T)$ using FMR; \circ —data from neutron diffraction.⁶²

ture dependence of the spontaneous magnetic moment $M_0(T)$ at zero internal field for K_2CuF_4 . In Fig. 8(b) we show our measurements of the function $M_0(T)$, along with data obtained in experiments using neutron diffraction.⁶²

IV. A DESCRIPTION OF THE PHASE DIAGRAMS OF 2D-FERROMAGNETS IN A FIELD PERPENDICULAR TO THE PLANES

Let us turn to a theoretical description of the phase diagrams (Fig. 2) shown in Sec. II. Following the approach used in Refs. 63–65, it is convenient to investigate the behavior of the spin system at different scales.

The measured phase transition curves $H_c(T)$ and the temperature dependence of the easy-axis anisotropy $H_A(T)$ (see Fig. 2) in 2D ferromagnets can be related to the existence of a characteristic scale $R_1 \approx (J/A)^{1/2}$ (here and in what follows all dimensions are given in units of the in-plane lattice constant), over which the behavior of the magnetic system varies significantly. At small scales $R < R_1$ the rather small ($A \ll J$) easy-plane anisotropy is only weakly reflected in the spin fluctuations and need not be taken into account. Therefore, over scales $R < R_1$ the compounds $CuCl$ and K_2CuF_4 can be described in terms of the 2D Heisenberg ($2D-H$) model, in which the order parameter has three components ($n = 3$) (see Fig. 9).

Let us take spin fluctuations into account at these scales by using the renormalization group. In Refs. 63, 64 it was shown that when averaging is performed over the rapidly varying spin fluctuations at scales smaller than R , the Hamiltonian of a Heisenberg FM with the “easy plane” type of anisotropy (1) does not change its form if on a scale R we introduce an effective temperature T_R , anisotropies A_R, a_R , and an interlayer exchange interaction J'_R [in this case we say that we have “renormalized” the Hamiltonian (1)]. The effective parameters of the Hamiltonian (1) on a scale R are determined by the equations

$$\begin{aligned} T_R &= T Z_R^{-1}(T) + o\left(\left(\frac{T}{2\pi J}\right)^2\right) \\ A_{R,\text{exc}} &= A_{\text{exc}} Z_R^2(T), \quad A_{R,\text{dip}} = A_{\text{dip}} Z_R(T), \\ a_R &= a Z_R^2(T), \quad J'_R = J' Z_R(T), \end{aligned} \quad (6)$$

where the renormalization factor is

$$Z_R(T) = 1 - \frac{T}{2\pi J} \ln R. \quad (6a)$$

Hence, the only effect of including spin waves with wave vectors $q \gg R^{-1}$ on a scale R is the introduction of the effective temperature and anisotropy parameters (6): the mag-

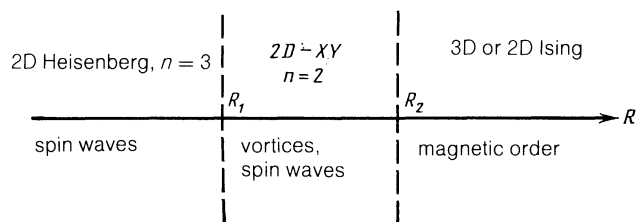


FIG. 9. Behavior regimes for an easy-plane 2D ferromagnet at different scales R : $R_1 \approx (J/A)^{1/2}$ and $R_2 \approx (J/J')^{1/2}$ are the characteristic scales in the system.

netic properties of the FM on new scales are described by starting not with the original parameters T, A, a, J' but rather with the new renormalized T_R, A_R, a_R, J'_R . We note that according to (6) the exchange and dipole parts of the easy-plane anisotropy constant A are renormalized differently.^{63,65} The contribution from the dipole-dipole interaction to the uniaxial anisotropy energy in the easy-magnetization plane a is small.⁵⁷ The magnetic field H in the Heisenberg model is not renormalized. The magnetic moment of a block of spins of size R in a Heisenberg FM is determined in Refs. 63, 64:

$$M_R = M_0 Z_R(T). \quad (6b)$$

More precisely, including further terms in $T/2\pi J$ the renormalization of the temperature is determined from the equation in Ref. 66:

$$\frac{dT_R}{d(\ln R)} = \frac{T_R^2}{2\pi J} \left(1 + \frac{T_R}{2\pi J} \right). \quad (6c)$$

The Heisenberg renormalization is cut off at a scale

$$R = R_1 = \min\{(T_R/A_R)^{1/2}, (J/A_R)^{1/2}\}. \quad (7)$$

At scales $R \gg R_1$ the anisotropy energy $E_A = A_R R^2$ exceeds the exchange energy J (or the temperature T_R which determines the characteristic energy at low temperatures where $T_R < J$) and the spins are “stacked” in the plane. On these scales the fluctuations of the order parameter become effectively two-dimensional; they take place only in the plane, so that $\langle m_z(R) m_z(0) \rangle \approx 0$ and the magnetic system goes over into the two-dimensional XY regime⁶⁴ (see Fig. 9). Further into this regime the system can be described by the BKT theory with effective parameters T_R and A_R , which can be found from (6) if we set $R = R_1$ in (6a):

$$Z_R(T) = 1 - \frac{T}{2\pi J} \ln\left(\frac{J}{A_R}\right). \quad (8)$$

At low temperatures ($T_R < J$) it is necessary to replace J by T_R in the logarithm appearing in (8).

On scales $R > R_1$ there exists a new type of excitation in addition to the spin waves, the magnetic vortex. Magnetic vortices have a core of size R_1 (Refs. 5, 9) and are fully analogous to vortices in superfluids.⁴ At low temperatures vortices with opposite circulations are joined in bound pairs. At a temperature $T = T_{\text{BKT}}$ the free energy of an isolated vortex goes to zero; this results in a phase transition associated with the dissociation of a portion of the vortex pairs (i.e., the Berezinski-Kosterlitz-Thouless transition¹⁻³), and a finite density of free vortices appears in the 2D system. In the XY -model, neglecting the interaction of vortex pairs, the BKT transition temperature is determined by the simple expression

$$T_{\text{BKT}} = \frac{\pi}{2} J = \pi S^2 J_0. \quad (9)$$

There is a significant difference between the systems under study here, which exhibit easy-plane anisotropy, and the XY model. First of all, the Heisenberg renormalization (6), (8) due to spin waves at scales $R \leq R_1$ must be included. Secondly, in contrast to the case where the external field is directed in the easy-magnetization plane, a field perpendicular to this plane cannot immediately destroy the BKT transition. In

this case the spins turn toward the direction $\mathbf{H} \parallel \mathbf{z}$ and the projection of the spins \mathbf{S}_{\parallel} decreases; because of this the BKT transition is shifted toward the region of lower temperatures [see (10)]. Hence, an entire curve of BKT transitions appears on the H - T phase diagram of a planar 2D ferromagnet.³²

This curve of BKT transitions can be found in the following way. The magnetic field \mathbf{H} perpendicular to the spin layers decreases the effective component \mathbf{S}_{\parallel} . Using the renormalized parameters on scales $R > R_1$, we find that

$$(S_{\parallel}/S)^2 = 1 - (S_z/S)^2 = 1 - (\hbar/A_R)^2, \quad (10)$$

where

$$\hbar = g\mu_B SH.$$

Only the spin projections in the plane \mathbf{S}_{\parallel} participate in the formation of vortex excitations (Fig. 10). As the field increases, the vortex excitation energy $E_{\text{vor}} \sim \pi JS_{\parallel}^2$ decreases along with \mathbf{S}_{\parallel} , which causes the BKT transition to occur at lower temperatures. Taking into account (9), (10) and also (6), (8), we find the BKT transition takes place at³²

$$T_R = \frac{\pi}{2} J \left[1 - \left(\frac{\hbar}{A_R} \right)^2 \right]. \quad (11)$$

We will use this equation [compare with (9)] to describe phase transitions in 2D ferromagnets such as CuCl1 and K_2CuF_4 .

The contribution of Heisenberg fluctuations to the destruction of magnetic order determines the temperature dependence of the anisotropy field $H_A(T)$ (Fig. 2, see Sec. II). An external field $H \approx H_A(0)$ perpendicular to the planes will completely expel the spins from the easy magnetization plane and turn them in the direction of the difficult-magnetization axis, i.e., $\mathbf{S}_{\parallel} = 0$. In this case the vortex excitations disappear (because $\mathbf{S}_{\parallel} = 0$ at the scale $R = R_1$), while the spin fluctuations with scales $R > R_1$ can be neglected. Under these conditions the measured temperature dependence $H_A(T)$ (see Sec. II) is determined only by the Heisenberg spin waves on small scales $R < R_1$. A further increase in the field affects the magnetic order only weakly. This is confirmed by the following experimental result: for $H \gtrsim H_A(0)$ the dependence of the FMR spectrum on field is close to linear (see Fig. 1):

$$\nu(H) \approx \nu_z(H - H_A(T)) \sim \hbar - A_R, \quad (12)$$

where the renormalization parameter for the easy-plane anisotropy A_R determined from Eqs. (6), (8) leads to

$$H_A(T) = H_{A,\text{exc}} Z_R^2(T) + H_{A,\text{dip}} Z_R(T). \quad (13)$$

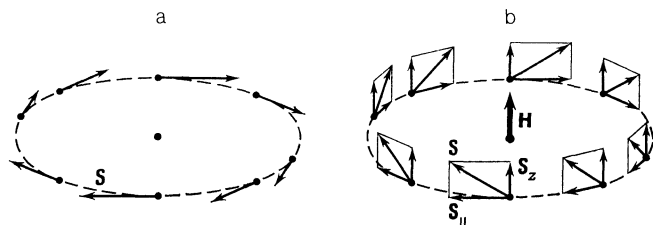


FIG. 10. Spin vortex in an easy-plane 2D ferromagnet for a magnetic field $\mathbf{H} \parallel \mathbf{z}$: a— $H = 0$; b— $0 < H < H_A$.

In large fields $H \gg H_A$ the Heisenberg characteristic scale decreases like $R_1 \approx (J/(H - H_A))^{1/2}$. As the field increases, this leads to an unusual enhancement of the value of the field anisotropy H_A (and also M_z) at fixed temperature; however, a significant variation in the magnitude of H_A should be observed only within a range of fields on the order of the exchange fields $H_E \gg H_A$.

The curves in Fig. 2 which describe the functions $H_A(T)$ for both the compounds under study are plotted using Eq. (13), taking (8) into account. The values of the exchange constants and the anisotropy field $H_{A,\text{dip}}$ are taken from Table I. The field anisotropy H_A at $T = 0$ is determined from the extrapolations of $H_A(T)$ and $H_c(T)$ (see Fig. 2, Sec. II).

As we have already noted in Sec. II, the function $H_A(T)$ in Fig. 2 does not correspond to any real phase transition in a 2D ferromagnet. The curves $H_A(T)$ have the following physical meaning: in a system in which there were no vortex excitations (e.g., in 3D ferromagnets or in easy-axis 2D ferromagnets), only spin waves, the phase transition would take place near the curve $H_A(T)$, which also is determined by the contribution of spin waves alone to the destruction of order in the planes. However, in the easy-plane 2D ferromagnets, the dissociation of vortex pairs induces a phase transition in a field $H_c(T)$ less than $H_A(T)$. Hence, the difference between $H_c(T)$ and $H_A(T)$ in the FM under study is essentially caused by vortex excitations.

After determining $A_R = H_A(T)$ we can calculate the BKT transition curve on the H - T diagram by using Eq. (11) and taking into account (6), (8), without fitting parameters (Fig. 2). The following values of the BKT temperatures in a field $H = 0$ are obtained within this calculation scheme: $T_{\text{BKT}} = 8.4$ K for CuCl1 and $T_{\text{BKT}} = 5.7$ K for K_2CuF_4 , respectively. Our estimate of the BKT temperature in K_2CuF_4 is found to be in good agreement with the results of Refs. 25–28, where a value of $T_{\text{BKT}} = 5.5$ K was obtained. The BKT curves in Fig. 2 show that a BKT vortex transition should occur in the compounds under study in the absence of the interplane interaction J' and intraplane anisotropy a . In the real magnetic systems CuCl1 and K_2CuF_4 the nonzero values of J' and a (although they are very small; see Table I) change the character of the BKT transition, so that long-range ferromagnetic order appears in these compounds with a spontaneous magnetic moment $\mathbf{M}_{\parallel} \neq 0$ at a temperature $T_c(H)$ which is somewhat higher than the $T_{\text{BKT}}(H)$ obtained from the BKT theory and based on (11). The phase transition temperature shift

$$\Delta T_c(H) = T_c(H) - T_{\text{BKT}}(H)$$

can be estimated as in Ref. 9.

The interactions J' , a form still another characteristic scale on which the magnetic system changes its behavior

$$R_2 \approx \min \{ (J/J')^{1/2}; (J/a)^{1/2} \}$$

(see Fig. 9). At scales $R > R_2$ the vortex excitations are suppressed. As the BKT transition is approached from the high-temperature side, the spin correlation radius $\xi(T)$ in the plane increases according to Refs. 4, 9:

$$\xi(T) \approx \exp(bt^{-1/2}), \quad T \geq T_{\text{BKT}}, \quad (14)$$

where

$$t = (T - T_{\text{BKT}}) / T_{\text{BKT}}, \quad b \approx \pi/2.$$

As the temperature decreases we eventually reach $\xi(T) \approx R_2$, at which point the interplanar exchange J' or the in-plane anisotropy a will bring the system into the 3D or 2D Ising regimes, respectively (i.e., a so-called "crossover" takes place). In both cases three-dimensional ferromagnetic order develops in the system with $\mathbf{M}_{\parallel} \neq 0$ at a value of temperature $T = T_c(H)$, where

$$R_2 \approx \xi(T) \approx \exp[b(T_{\text{BKT}}(H) / \Delta T_c(H))^{1/2}]. \quad (15)$$

Hence, the critical curve for real phase transitions is determined by the equation

$$T_c(H) = T_{\text{BKT}}(H) \left[1 + \left(\frac{b}{\ln R_2} \right)^2 \right] \sim T_{\text{BKT}}(H). \quad (16)$$

From Eq. (16) we can obtain only estimates of the magnitude of the shift of the phase transition temperature: $T_c - T_{\text{BKT}} = 0.9$ K and 0.8 K for CuCl1 and K_2CuF_4 , respectively. However, this is already found to be in rather good agreement with the measured T_c (see Table I). On the other hand, from (16) it follows that the critical temperature $T_c(H)$ as a function of field is proportional to the temperature $T_{\text{BKT}}(H)$. Using this fact, we obtained the theoretical curves $T_c(H)$ shown in Fig. 2, which describe the measured curves of phase transitions, from the BKT curves according to (16) such that the value $T_c(0)$ in zero field coincides with the real ferromagnetic transition temperatures $T_c = 8.8$ K and 6.25 K for CuCl1 and K_2CuF_4 respectively (see Table I).

V. DESCRIPTION OF THE TEMPERATURE DEPENDENCE OF VARIOUS MAGNETIC CHARACTERISTICS IN TERMS OF SIMILARITY THEORY

Let us now turn to a theoretical description of the temperature dependence of the magnetic characteristics $M_0(T)$, $H_a(T)$, and $\nu_0(T)$ (see Figs. 6,8), determined from the FMR spectrum in the case where the external field is parallel to the easy axis ($\mathbf{H} \parallel \mathbf{z}$). For $H = 0$ the density of vortex pairs n_{vor} is small over the entire range of temperatures $T \lesssim T_c$, so that the energy satisfies $E_{\text{vor}} \propto \pi J$ and

$$n_{\text{vor}} \propto \exp(-E_{\text{vor}} / k_B T) \ll 1.$$

A magnetic field $\mathbf{H} \parallel \mathbf{z}$ does not decrease the vortex energy (as is the case for $\mathbf{H} \parallel \mathbf{z}$, see Sec. IV), but rather increases it, which in turn decreases the vortex density. Therefore, when we analyze the temperature dependence of $M_0(T)$, $H_a(T)$, and $\nu_0(T)$ measured in the geometry $\mathbf{H} \parallel \mathbf{z}$, we can neglect entirely the extremely small vortex density over the entire range $T \lesssim T_c$ and include only the spin-wave excitations. An appreciable vortex density arises only near T_c , where the free energy of the vortices (by virtue of the increase in their anisotropic part) approaches zero.⁴ Let us examine once again that in an external field perpendicular to the easy plane the situation is otherwise (see Sec. IV): the magnetic field decreases the vortex energy at any temperature $T \lesssim T_c$ (by virtue of the decrease in the in-plane spin projection \mathbf{S}_{\parallel} which makes up the vortex excitation, Fig. 9), so that near the BKT curve (Fig. 2) an appreciable vortex density arises.

The temperature dependence of any of the magnetic characteristics (in particular, $M_0(T)$, $H_a(T)$, and $\nu_0(T)$) is easily obtained from considerations of similarity (i.e., scale

invariance of two-dimensional degenerate systems), following Ref. 67. At this point we will continue our investigation of the behavior of easy-plane 2D ferromagnets on different scales which we started in Sec. IV. "Starting" with the atomic scales, where the parameters of magnetic systems are known and coincide with the $T = 0$ parameters (see Table I), we pass to successively larger sizes of spin blocks while averaging over the short-range fluctuations within the blocks until we arrive at macroscopic scales (see the scheme in Fig. 9). The macroscopic magnetic quantities obtained in this way will also correspond to the characteristics of $M_0(T)$, $H_a(T)$, and $\nu_0(T)$ measured in FMR experiments.

In Sec. IV it was shown that up to scales $R \leq R_1 \approx (J/A)^{1/2}$ [for more precision see (7)] the spin fluctuations are three-component and these 2D systems are described by the Heisenberg model (see the scheme in Fig. 9). At distances $R \approx R_1$ the easy-plane anisotropy "stacks" the spins in the plane, and the spin fluctuations become effectively two-component (we can neglect the fluctuations m_z). Averaging over smooth-scaled fluctuations (i.e., with respect to spin waves with wave vectors $q < R^{-1}$) within the framework of the renormalization group approach reduces on scales $R > R_1$ to substituting for the original parameters of the magnetic Hamiltonian (1) the effective (renormalized) parameters T_R , A_R , a_R , J'_R , and M_R (6) (Refs. 61–63).

In what follows we will use the results obtained in Refs. 67 and 5. According to Ref. 67, for the case of planar 2D ferromagnets considerations of scale invariance are applicable in the large-distance regime not only at the transition point itself but also for all temperatures $T < T_c$. Therefore the sought-after temperature dependences $M_0(T)$, $H_a(T)$, and $\nu_0(T)$ in these systems can be found by using scaling transformations at distances $R \gg R_1$. Thus, e.g., in order to find the temperature dependence of the magnetic moment $M_0(T)$ we introduce the scaling dimension Δ_M for this quantity. This implies that for a scale transformation $R \rightarrow lR$ the quantity $M(R)$ transforms according to the law⁶⁵

$$M(lR) = l^{-\Delta_M} M(R). \quad (17)$$

Analogously we can introduce scaling dimensions for all of the other quantities: Δ_H for magnetic field, Δ_a for the intraplanar anisotropy constant, Δ_J for the interlayer exchange, etc.. The scaling dimensions of different quantities were also found by the authors of Ref. 67 from general similarity relations:

$$\Delta_M = \Delta = \frac{T_R}{4\pi J}, \quad \Delta_H = \Delta, \quad \Delta_a = 4\Delta, \quad \Delta_J = 2\Delta. \quad (18)$$

In contrast to Ref. 67, the scaling exponents we present here are for transforming not the anisotropy energy, field, etc., but rather the constants for these interactions which enter into the Hamiltonian (1). In (18) the Heisenberg renormalization (6), (8) at small scales is also taken into account.

As we have already noted briefly in Sec. IV, the interaction between J' planes are the in-plane anisotropy a form a second characteristic scale

$$R_2 \approx \min\{(J/J')^{1/2}, (J/a)^{1/2}\},$$

at which the systems pass from the 2D – XY to the 3D- or 2D-Ising regimes (see Fig. 9). In both cases the spin fluctuations are suppressed on scales $R \gg R_2$ and the characteristics

of the magnetic systems cease to change. This implies that the spin waves with $q < R_2^{-1}$ contribute practically nothing to the temperature behavior of the magnetic characteristics of these systems. Hence, in order to determine the temperature dependence of any quantity it is necessary to pass from the scale $R = R_1$, where the effective parameters of the system are determined by Eqs. (6), (8) (see Sec. IV), to the scale R_2 at which the spin system "freezes", by means of the scale transformation (17), (18). Thus, e.g., for $M(T)$ we have

$$M(T) = M_{R_2} = (R_2/R_1)^{-\Delta} M_{R_1} \quad (19)$$

The second characteristic scale R_2 we can determine more accurately if we take into account the fact that at the dimensions of a spin block R_2 the intraplanar anisotropy energy a_{R_2} or the interlayer exchange J'_{R_2} become on the order of the temperature T_R (or J for $T \gg J$):

$$E_a(R_2) = a_{R_2} R_2^2(a) = T_R$$

or

$$E_{J'}(R_2) = J'_{R_2} R_2^2(J') = T_R.$$

From this, taking (18), (19) into account, it follows that the uniaxial anisotropy a in the plane and the three-dimensional exchange J' define the following characteristic scales:

$$R_2(a)/R_1 = (A_R/a_R)^{1/(2-\Delta)} \quad (20a)$$

$$R_2(J')/R_1 = (A_R/J'_R)^{1/(2-2\Delta)} \quad (20b)$$

where the ratio R_2/R_1 entering into (19) is obtained by taking (7) into account. Then when $a \neq 0$ and $J' \neq 0$ at the same time, ferromagnetic order is established on the scale

$$R_2 = \min\{R_2(a); R_2(J')\}. \quad (20c)$$

Now we can determine the sought-after temperature dependences $M_0(T)$, $H_a(T)$, and $\nu_0(T)$ by means of the scale transformation (17), (18) and taking into account (20) and (6):

$$M_0(T) = (R_2/R_1)^{-\Delta} M_{R_1} = M_0 Z_R(T) (R_2/R_1)^{-\Delta}, \quad (21a)$$

$$a(T) = (R_2/R_1)^{-\Delta} a_R = a Z_R^2(T) (R_2/R_1)^{-\Delta}, \quad (21b)$$

$$\nu_0(T) = \nu_0 [a(T) A_R(T) / a A]^{1/2}. \quad (21c)$$

In the course of describing the functions $\nu_0(T)$ and $H_a(T)$ determined from experiment (see Sec. III) it is necessary to make the following additional observations:

(1) At $H = 0$ the demagnetizing field of the sample contributes to the FMR frequency [see (2)]. Therefore in calculating the measured function $\nu_0(T)$ in a CuCl1 crystal (see Fig. 4) we used not (21c) but the expression

$$\nu(T) = \nu_0 \left[\frac{a(T)}{a} \left(\frac{A_R(T) + (N_z - N_{||}) M_0(T)}{A + (N_z - N_{||}) M_0} \right) \right]^{1/2}; \quad (22)$$

(2) The intraplanar anisotropy field H_a in CuCl1 was determined from the measured field at which the reorientation transition occurred in the easy plane and the magnetic moment fully rotated in the plane from the easy magnetization axis to the field direction (see Sec. III). Therefore our experiment measured not the intraplane anisotropy constant $a(T)$ itself, but rather the magnetic field $H_a(T)$ which balances the effect of the in-plane anisotropy at large scales (on the order of R_2). Consequently, taking into account the scal-

ing transformations (18), (19) for the field constant and (21b), $H_a(T)$ is determined by the equation

$$H_{R_2} = H_a(T) (R_2/R_1)^{-\Delta} = a_{R_2} = a(T), \quad (23)$$

from which

$$H_a(T) = H_a Z_R^2(T) (R_2/R_1)^{-3\Delta}. \quad (24)$$

As a consequence of the compensation of the intraplanar anisotropy in an external field, the characteristic scale R_2 in (24) involves only the interlayer exchange J' . Therefore in describing the measured function $H_a(T)$ (Fig. 4) with Eq. (24), we set $R_2 = R_2(J')$ from (20b) in this expression.

At lower temperatures $T \ll J$, Eqs. (21a), (21b), and (24) found from considerations of scale invariance naturally pass over into expressions which can be obtained from standard spin-wave calculations (see e.g., Ref. 68):

$$\begin{aligned} M_0(T) &= M_0 \left[1 - \frac{T}{4\pi J} \ln \left(\frac{k_B T}{g\mu_B S (H_a H_A)^{1/2}} \right) \right], \\ \nu_0(T) &= \nu_0(0) \left[1 - \frac{T}{2\pi J} \ln \left(\frac{k_B T}{g\mu_B S (H_a H_A)^{1/2}} \right) \right], \\ H_a(T) &= H_a(0) \left[1 - \frac{T}{2\pi J} \ln \left(\frac{k_B T}{g\mu_B S H_A^{1/2} H_e^{3/2}} \right) \right]. \end{aligned} \quad (25)$$

The spin-wave relations (25), which include only the terms which are linear in $T/2\pi J$, in principle already describe the temperature dependences of the magnetic characteristics fairly well (i.e., their features at low temperatures $T \lesssim 0.5T_c$). On the other hand, Eqs. (22), (24), and (21a), which were obtained within the framework of similarity theory, in fact include subsequent terms in $T/2\pi J$ exactly [under the conditions that the renormalization of the temperature is calculated from (6c)]. Therefore, for a more accurate description of the experimental results obtained here over the wide temperature interval $T \lesssim T_c$, we use the relations (22), (24) and (21a). The theoretical curves which describe the experimental data for $\nu_0(T)$ and $H_a(T)$ for CuCl1 in Fig. 6 and $M_0(T)$ for K_2CuF_4 in Fig. 8 were calculated using Eqs. (22), (24), and (21a), respectively, in which the renormalization factor $Z_R(T)$ was chosen from (8) and the values of the characteristic scales R_1, R_2 from (7) and (20). In carrying out the calculations, the in-plane exchange constant J and the easy-plane anisotropy field H_A for both compounds, and also the value of the interlayer exchange $J'(H_a)$ for K_2CuF_4 , were chosen from Table I. The remaining parameters entering into the expressions were chosen for the best fit: (1) $H_a = 86 \pm 2$ Oe and $H_e = 35 \pm 5$ Oe for the best description of $H_a(T)$ for CuCl1 (see Fig. 6); (2) $\nu_0 = 1240 \pm 20$ MHz at $T = 0$ for CuCl1 (Fig. 6); (3) $M_0 = 99 \pm 2$ Oe for K_2CuF_4 (Fig. 8). The results obtained for these constants are found to be in full agreement with the data obtained in other papers (see Table I). The theory of similarity of 2D ferromagnets^{67,5} has allowed us to arrive at a good description of the measured functions $H_a(T)$ and $\nu_0(T)$ for CuCl1 and $M_0(T)$ for K_2CuF_4 in the broad temperature range up to $T \approx T_c$ (Figs. 6,8) with practically no fitting parameters (all values of the constants which were chosen in the calculations either coincide completely or render somewhat more precise the data given in Table I). We note that Eq. (25), which can be obtained from spin-wave theory, gives satisfactory agreement with experiment only

up to temperatures ≈ 3 K. Hence, the theory of similarity for two-dimensional degenerate systems, in contrast to spin-wave theory, gives good agreement with experiment without cumbersome calculations not only at low temperatures but also over the broad temperature range up to $T \approx T_c$.

CONCLUSIONS

In this paper we have obtained the following basic results:

(1) We have measured the FMR spectrum in the quasi-two-dimensional easy-plane ferromagnets $(\text{CH}_3\text{NH}_3)_2\text{CuCl}_4$ and K_2CuF_4 in the frequency range 100 to 4500 MHz and temperature range 1.2 to 20 K for various directions of the magnetic field.

(2) We have observed that, in contrast to the usual 3D ferromagnets, when these 2D ferromagnets are subjected to a magnetic field perpendicular to the easy-magnetization plane, the phase transition field $H_c(T)$ is found to be smaller than the easy-plane anisotropy field $H_A(T)$. We have determined the temperature dependence of the fields $H_c(T)$ and $H_A(T)$ on the H - T diagram from the FMR spectra in this geometry for both compounds.

(3) The measured H - T phase diagrams can be quantitatively described using the theory of Berezinski, Kosterlitz and Thouless, including the contribution to the destruction of magnetic order from spin waves and vortices.

(4) From the FMR spectra measured in a magnetic field parallel to the easy-magnetization plane, we found the temperature dependence of the intraplanar anisotropy field and the FMR frequency at $H = 0$ for $(\text{CH}_3\text{NH}_3)_2\text{CuCl}_4$, and also the spontaneous magnetic moment $M_0(T)$ for K_2CuF_4 .

(5) From considerations of scale invariance for planar 2D ferromagnets⁶⁷ we have obtained a description of the measured functions $H_a(T)$, $\nu_0(T)$, and $M_0(T)$ over a wide region of temperatures $T \lesssim T_c$.

(6) In K_2CuF_4 we observed the existence of a gap in the FMR spectrum, amounting to $\nu_0 = 1370$ MHz at $T = 1.2$ K.

The authors are sincerely grateful to A. S. Borovik-Romanov for valuable advice and useful discussions, to V. L. Pokrovski and G. V. Uimin for assistance with the theoretical description of the experimental results, to A. V. Chubukov for verifying the theoretical calculations in the low-temperature limit and for critical remarks, and to A. N. Bazhan for carrying out the magnetization measurements.

¹V. L. Berezinski, Zh. Eksp. Teor. Fiz. **59**, 907 (1970) [Sov. Phys. JETP **32**, 493 (1970)]; Zh. Eksp. Teor. Fiz. **61**, 1144 (1971) [Sov. Phys. JETP **34**, 610 (1971)].

²J. M. Kosterlitz and D. J. Thouless, J. Phys. C **6**, 118 (1973).

³J. M. Kosterlitz, J. Phys. C, **7**, 1046 (1974).

⁴J. M. Thouless and D. J. Thouless, Prog. Low Temp. Phys. **7B**, 373 (1978).

⁵A. Z. Patashinskii and V. L. Pokrovskii, *Fluktuatsionnaya teoriya fazovykh perekhodov (Fluctuation Theory of Phase Transitions)*, Pergamon, Oxford, 1979), Moscow: Nauka, 1982.

⁶J. Vilain, J. de Phys. **36**, 581 (1975).

⁷J. V. Jose, L. P. Kadanoff, S. Kirkpatrick, and D. R. Nelson, Phys. Rev. B **16**, 1217 (1977).

⁸D. R. Nelson and J. M. Kosterlitz, Phys. Rev. Lett. **40**, 1727 (1978).

⁹S. Hikami and T. Tsuneto, Prog. Low Temp. Phys. **63**, 387 (1980).

¹⁰D. S. Bishop and J. D. Reppy, Phys. Rev. Lett. **40**, 1721 (1978); Phys. Rev. B **22**, 5171 (1980).

¹¹I. Rudnick, Phys. Rev. Lett. **40**, 1454 (1978).

¹²J. Maps and R. B. Hallock, Phys. Rev. Lett. **40**, 1533 (1981).

¹³G. Agnolet, S. L. Teitel, and J. D. Reppy, Phys. Rev. Lett. **47**, 1537 (1981).

¹⁴D. Finotello and F. M. Gasparini, Phys. Rev. Lett. **55**, 2156 (1985).

¹⁵M. R. Beasley, J. E. Mooij, and T. P. Orlando, Phys. Rev. Lett. **42**, 1165 (1979).

¹⁶S. A. Wolf, D. U. Gubser, W. W. Fuller, J. C. Garland, and R. S. Newrock, Phys. Rev. Lett. **47**, 1071 (1981).

¹⁷K. Epstein, A. M. Goldman, and A. M. Kadin, Phys. Rev. B **28**, 3950 (1983).

¹⁸A. T. Fiory, A. F. Hebard, and W. I. Glaberson, Phys. Rev. B **28**, 5075 (1983).

¹⁹A. Schenstrom, M. Levy, H. P. Fredricksen, and J. Gavaler, Physica B **135**, 128 (1985).

²⁰M. Suzuki, S. Miyashita, A. Kuroda, and C. Kawabata, Phys. Lett. A **60**, 478 (1977).

²¹C. Kawabata and K. Binder, Solid State Commun. **22**, 705 (1986).

²²S. Miyashita, H. Nishimori, A. Kuroda, and M. Suzuki, Prog. Theor. Phys. **60**, 1669 (1978).

²³J. Tobochnik and G. V. Chester, Phys. B **20**, 3761 (1979).

²⁴C. Kawabata and A. R. Bishop, Solid State Commun. **60**, 169 (1986).

²⁵K. Hirakawa and K. Ubukoshi, J. Phys. Soc. Jpn. **50**, 1909 (1981).

²⁶K. Hirakawa, H. Yoshizawa, and K. Ubukoshi, J. Phys. Soc. Jpn. **51**, 2151 (1982).

²⁷K. Hirakawa, J. Phys. Soc. Jpn. **53**, 1893 (1982).

²⁸K. Hirakawa, H. Yoshizawa, J. D. Axe, and G. Shirane, J. Phys. Soc. Jpn. **52**, 4220 (1983).

²⁹L. P. Regnault, J. Rossat-Mignod, J. Y. Henry, and L. J. DeJongh, J. Magn. Magn. Mater. **31-34**, 1205 (1983).

³⁰L. P. Regnault, J. Rossat-Mignod, J. Y. Henry, R. Pynn, and D. Petitgrand, Springer Series in Solid-State Sciences **54: Magnetic Excitations and Fluctuations**, p. 201 (1984).

³¹L. P. Regnault, J. P. Boucher, J. Rossat-Mignod *et al.*, Physica B **136**, 329 (1986).

³²A. Abrikosov, Zh. Eksp. Teor. Fiz. **71**, 2402 (1976) [Sov. Phys. JETP **44**, 1266 (1976)].

³³M. Suzuki, J. Phys. Soc. Jpn. **51**, 2772 (1982).

³⁴L. J. DeJongh and A. R. Miedema, Adv. Phys. **23**, 1 (1974).

³⁵Yu. S. Karimov, Zh. Eksp. Teor. Fiz. **65**, 261 (1973) [Sov. Phys. JETP **38**, 129 (1973)].

³⁶J. H. P. Colpa, Physica **57**, 347 (1972).

³⁷I. Yamada, J. Phys. Soc. Jpn. **33**, 979 (1972).

³⁸A. Dupas and J. P. Renard, Phys. Rev. A **53**, 141 (1975).

³⁹S. O. Demokritov, N. M. Kreines, V. I. Kudinov, S. V. Petrov, and A. V. Chubukov, Zh. Eksp. Teor. Fiz. **94**, (12) 283 (1988) [Sov. Phys. JETP **67**, 2552 (1988)].

⁴⁰R. D. Willet, J. Chem. Phys. **41**, 2243 (1976).

⁴¹J. J. M. Steijer, E. Frikkee, L. J. DeJongh, and W. J. Huiskamp, Phys. B **123**, 271 (1984); Physica B **123**, 284 (1984).

⁴²M. Hidaka and P. J. Walker, Solid State Commun. **31**, 383 (1979).

⁴³I. Yamada, I. Morishita, and T. Tokuyama, Physica B **115**, 179 (1983).

⁴⁴G. Heygster and W. Kleemann, Physica B **89**, 165 (1977).

⁴⁵W. Kleemann and F. J. Schafer, J. Magn. Magn. Mat. **21**, 143 (1980).

⁴⁶S. Funahashi, F. Moussa, and M. Steiner, Solid State Commun. **18**, 433 (1976).

⁴⁷F. Mossa and J. Villain, J. Phys. C **9**, 4433 (1976).

⁴⁸K. Takeda, Y. Okuda, I. Yamada, and T. Haseda, J. Phys. Soc. Jpn. **50**, 1917 (1981).

⁴⁹L. J. DeJongh and W. D. Van Amstel, J. de Phys. Suppl. 2-3, **32**, 880 (1971).

⁵⁰H. Yamazaki, J. Phys. Soc. Jpn. **37**, 667 (1974).

⁵¹A. S. Borovik-Romanov, N. M. Kreines, R. Laiho, T. Levola, and V. G. Zhotikov, J. Phys. C **13**, 879 (1980).

⁵²T. Grieb, W. Kullmann, P. Fehr, K. Strobel, and R. Geick, J. Phys. C **17**, 6843 (1984).

⁵³H. Yamazaki, Y. Morishiga, and M. Chikamatsu, J. Phys. Soc. Jpn. **50**, 2872 (1981).

⁵⁴H. Yamazaki, J. Phys. Soc. Jpn. **41**, 1911 (1976).

⁵⁵P. Bloembergen and A. R. Miedema, Physica **75**, 205 (1974).

⁵⁶J. E. Drumheller, P. H. Amundson, and E. Emerson, J. Chem. Phys. **51**, 5729 (1969).

⁵⁷P. Bloembergen and A. R. Miedema, Physica **81**, 205 (1976).

⁵⁸E. A. Turov, *Fizicheskaya svoistva magnitouporyaochennykh kristallov (Physic Properties of Magnetically-Ordered Crystals)*, Academic, New York, 1965, Moscow, Izd. AN SSSR, 1963.

⁵⁹W.-H. Li, C. H. Rerry, J. B. Sokoloff *et al.*, Phys. Rev. B **35**, 1891 (1987).

⁶⁰A. S. Borovik-Romanov and E. G. Rubashevskii, Zh. Eksp. Teor. Fiz. **47**, 2095 (1964) [Sov. Phys. JETP **20**, 1407 (1964)].

⁶¹A. S. Borovik-Romanov, N. M. Kreines, and L. A. Prozorova, Zh. Eksp. Teor. Fiz. **45**, 64 (163) [Sov. Phys. JETP **18**, 46 (1963)].

⁶²K. Hirakawa and H. Ikeda, J. Phys. Soc. Jpn. **35**, 1328 (1973).

- ⁶³D. R. Nelson and R. A. Pelcovits, *Phys. Rev. B* **16**, 2191 (1977).
⁶⁴S. B. Khokhlachev, *Zh. Eksp. Teor. Fiz.* **70**, 265 (1976) [*Sov. Phys. JETP* **70**, 137 (1976)]; *Zh. Eksp. Teor. Fiz.* **71**, 812 (1976) [*Sov. Phys. JETP* **44**, 427 (1976)].
⁶⁵V. J. Pokrovskii and M. V. Feigel'man, *Zh. Eksp. Teor. Fiz.* **72**, 557 (1977) [*Sov. Phys. JETP* **45**, 291 (1977)].

- ⁶⁶E. Brezin and J. Zinn-Justin, *Phys. Rev. B* **14**, 3110 (1976).
⁶⁷V. L. Pokrovskii and G. V. Uimin, *Zh. Eksp. Teor. Fiz.* **65**, 1961 (1973) [*Sov. Phys. JETP* **38**, 847 (1973)].
⁶⁸K. Tsuru and N. Urya, *J. Phys. Soc. Jpn.* **41**, 804 (1976).

Translated by Frank J. Crowne